

# Jet-Studies and $\alpha_s$ -determinations at HERA\*

Gerd W. Buschhorn  
 Max-Planck-Institut für Physik  
 (Werner-Heisenberg-Institut)  
 Föhringer Ring 6  
 80805 München

## Abstract

Recent results from the H1 and ZEUS Collaborations on inclusive single and multiple jet production in the neutral current deep inelastic scattering of electrons/positrons on protons and the high energy photoproduction on protons at HERA are reported. The results are compared with NLO QCD calculations and have been used to determine the strong interaction coupling constant  $\alpha_s$ .

## 1 Introduction

The study of jets in the deep inelastic scattering (DIS) of electrons/positrons on protons and in high energy photoproduction on protons enables sensitive tests of QCD to NLO and provides precision measurements of the strong interaction coupling constant  $\alpha_s$ . In this report a survey is given of results from recent measurements of jet production in neutral current processes from the H1 and the ZEUS Collaborations at the HERA collider; not included in this review are results on jets associated with diffraction, heavy flavours or direct photons.

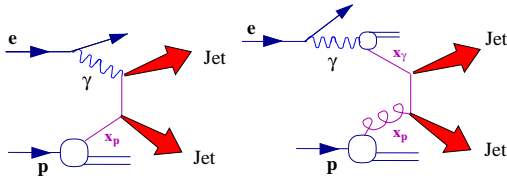


Figure 1: Examples of leading-order contributions to inclusive jet production: (left) direct photon interaction, (right) resolved photon interaction.

In jet studies QCD predictions for DIS and photoproduction are probed in different regions of the DIS variables (Bjorken)  $x$  and  $Q^2$  (with  $y = Q^2/sx$  and  $s$  the squared  $ep$  centre-of-mass energy) and the transverse energy  $E_T$  and pseudorapidity  $\eta_j$

\*Talk given on behalf of the H1- and ZEUS-Collaborations at the conference "New Trends in High-Energy Physics", Alushta, Crimea, Ukraine, May 24-31, 2003

(defined as  $\eta_j = -\log \text{tg } \Theta_j/2$  with  $\Theta_j$  the polar jet angle with respect to the proton beam) of the hadronic jet or jets. In DIS at high  $Q^2$  the virtual photon emitted from the electron interacts with a parton from the proton in a direct (pointlike) process while at low  $Q^2$  and in photoproduction it can fluctuate into partons, one of which interacts in so-called resolved processes with a parton of the proton (fig. 1).

In pQCD jet production depends on the hard partonic scattering process and on the parton density functions (PDFs) of the proton and, in photoproduction and low  $Q^2$  processes, also of the photon. For the calculation of the jet cross section  $\sigma_j$  in DIS (for photoproduction see Chap. 3), the hard partonic cross section  $d\sigma_a$  for a parton  $a$  has to be convoluted with the PDFs  $f_a$  of the proton

$$\sigma_j = \sum_a \int dx f_a(x, \mu_F^2) d\sigma_a(x, \alpha_s(\mu_R^2), \mu_R^2, \mu_F^2) \cdot (1 + \delta_{\text{hadr}}) \quad (1)$$

and corrected for hadronization effects. The dependence of the PDFs on the characteristic energy scale of the interaction is described by evolution equations i.e. for not too small  $x$  and  $Q^2$  by the DGLAP equations. The summed higher order contributions of this evolution, corresponding to multiple collinear gluon emissions of the interacting parton, are represented by parton cascade diagrams. The factorization theorem allows the soft (nonperturbative) part of these contributions to be absorbed in the PDFs while the hard part has to be accounted for in the perturbative part of the interaction, it defines the factorization scale  $\mu_F$ . Examples of LO contributions to DIS are shown in fig. 2. A breakdown of the DGLAP approximation is to be expected in the small  $x$  region, where  $\log 1/x$ -terms become larger than  $\log Q^2$ -terms; in this region, the BFKL evolution equation should give a better description of DIS. A kind of interpolation between these approximations is provided by the CCFM approach.

A preferred reference system for analyzing jet processes in DIS is the Breit system in which the

parton collides head-on with the timelike virtual photon:  $2x\mathbf{p}+\mathbf{q}=0$ . In the quark parton model (QPM) the hadron jet resulting from the backscattered quark emerges collinear with the proton remnant, whereas QCD hard processes are characterized by jets with high transverse momenta with respect to the proton remnants. Analyzing the hadronic final state in the Breit system therefore suppresses the QPM background.

The identification of jets is achieved by algorithms which are applied to the objects of the measurement i.e. the particle tracks and energy clusters that are registered by the detector. Different jet algorithms have been developed and applied to the HERA experiments but in recent years the "inclusive longitudinally invariant  $k_T$  cluster algorithm" (in the following: ILICA) has become the preferred one. The algorithm proceeds by calculating for each track or energy cluster  $i$  the quantity  $d_i$  and for each pair the quantity  $d_{ij}$ :

$$\begin{aligned} d_i &= E_{T,i}^2, \\ d_{ij} &= \min(E_{T,i}^2, E_{T,j}^2)(\Delta\eta_{ij}^2 + \Delta\phi_{ij}^2) \end{aligned} \quad (2)$$

where  $E_{T,i}$  is the transverse energy of a particle  $i$  and  $\Delta\eta_{ij}$  and  $\Delta\phi_{ij}$  are the differences in the pseudorapidity  $\eta$  and azimuthal angle  $\phi$  of  $i, j$  respectively; all these quantities are invariant under longitudinal boosts i.e. boosts in the direction of the proton beam (defined as  $+z$ -direction). If of all resulting  $\{d_i, d_{ij}\}$  the smallest one belongs to  $\{d_i\}$  it is kept as a jet and not treated further if it belongs to  $\{d_{ij}\}$  the corresponding tracks or clusters are combined to a single object. The procedure is repeated until all tracks or clusters are assigned to jets. The algorithm is infrared and collinear safe, and can be applied to measurements of DIS and photoproduction processes. It typically requires smaller hadronization corrections than other clustering algorithms.

For tests of QCD, the measured jet cross sections have to be compared with calculations performed (at least) to NLO. These partonic final states have to be combined with models for the development of the parton cascade and the hadronization. Models for the parton cascade are the parton shower model, implemented in HERWIG and LEPTO, and the dipole cascade model, implemented in ARIADNE; the hadronization of the partons is modelled by the cluster model, implemented in HERWIG, or by the string fragmentation model, implemented in JETSET and used in LEPTO and ARIADNE. In RAPGAP the LO QCD matrix elements are matched to DGLAP based parton showers in the LL approximation; it allows RAPGAP, besides simulating direct processes, also the simulation of resolved photon processes. In CASCADE, the QCD matrix elements are combined with parton emissions described by the CCFM evolution equation with the

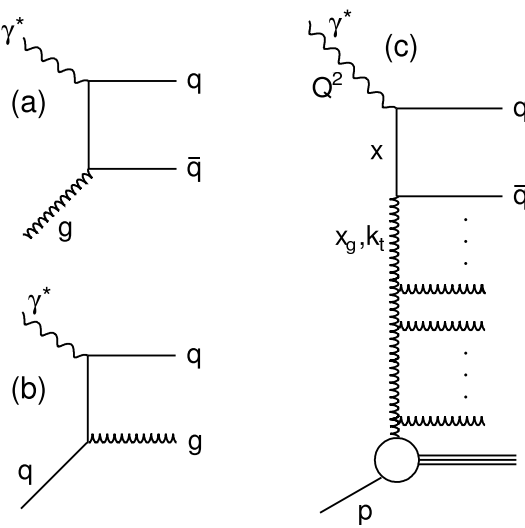


Figure 2: Leading order diagrams for (di)jet production: (a) photon-gluon fusion; (b) QCD-Compton process; (c) parton cascade.

unintegrated gluon density distribution used as input.

In photoproduction, direct and resolved interactions are simulated with PYTHIA, HERWIG and PHOJET. The hard partonic interaction is described by LO QCD matrix elements and the parton cascade is simulated by initial and final state parton showers in the LL approximation. In PYTHIA and PHOJET, the hadronization is simulated with the Lund string model as implemented in JETSET; in HERWIG the cluster model is used.

Commonly used parametrizations for the PDFs of the proton are those of CTEQ and MRST, while for the photon PDFs the GRV and AFG sets are used.

## 2 Jets in deep inelastic scattering

Results on inclusive jet production in DIS have been obtained on single jets, dijets and trijets and recently also on subjets. Since jet production at small  $x$  in the forward direction is related to forward single hadron production, results on  $\pi^0$ -production are also discussed.

### 2.1 Inclusive jets

At high  $Q^2$ , i.e. for  $150 \text{ GeV}^2 < Q^2 < 5000 \text{ GeV}^2$ , the inclusive jet cross section has been measured by H1 [1] in the Breit frame as a function of the jet transverse energy  $E_T$  for  $7 \text{ GeV} < E_T < 50 \text{ GeV}$ ,  $0.2 < y < 0.6$  and  $-1 < \eta_{\text{lab}} < 2.5$ . Jets were identified using the ILICA. Over the whole range of  $E_T$  and  $Q^2$ , the NLO calculation corrected for

hadronization effects ( $< 10\%$ ) gives a good description of the data (fig. 3).

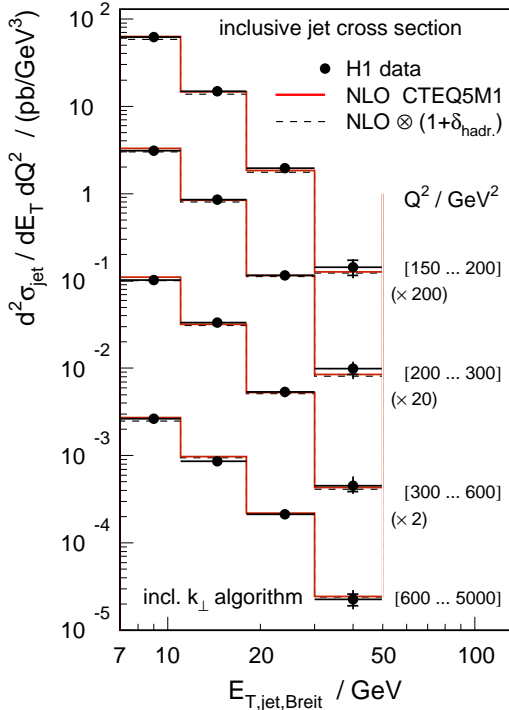


Figure 3: Inclusive jet cross section in DIS as fct. of the transverse jet energy in the Breit system  $E_{TjB}$ .

Fitting the QCD prediction to these cross sections using CTEQ5M1,  $\mu_R = E_T$  and  $\mu_F = \sqrt{200 \text{ GeV}^2}$  (the average  $E_T$  of the jet sample) yields  $\alpha_s$ . First in separate fits to the data points in the four  $Q^2$  regions  $\alpha_s(E_T)$  was determined and evolved to  $\alpha_s(M_Z)$ . The consistency of these fits justified a combined fit to all data points with the final result, taking into account the uncertainties of the renormalization scale ( $\mu_R = E_{Tj}$ ) and from the parton parametrization, of  $\alpha_s(M_Z) = 0.1186 \pm 0.0030(\text{exp}) + 0.0039/ - 0.0045(\text{theor}) + 0.0033/ - 0.0023(\text{PDF})$ . The experimental error is dominated by the hadronic energy scale of the LAr calorimeter with the statistical error contributing only 0.0007; the theoretical uncertainty includes about equal contributions from the hadronization and renormalization scale uncertainty. The result has been shown to be stable against variations of the jet algorithm.

Similar measurements have been performed recently by ZEUS [2]. For  $Q^2 > 125 \text{ GeV}^2$ ,  $E_{TB} > 8 \text{ GeV}$ ,  $-2 < \eta_{jB} < 1.8$  and demanding for the angle  $\gamma$  of the hadronic system  $-0.7 < \cos_\gamma < 0.5$ , the  $Q^2$ - and  $E_{TB}$ -dependence of the inclusive jet cross section is found to be in good agreement with NLO QCD calculations.

For the determination of  $\alpha_s$ , the differential cross sections  $d\sigma/dV$ , where  $V = Q^2, E_{TBj}$ , were calculated in NLO QCD for three MRST99 sets

i.e. central,  $\alpha_s \uparrow\uparrow$  and  $\alpha_s \downarrow\downarrow$ , taking for the partonic cross sections the  $\alpha_s(M_Z)$  of the corresponding PDFs. For each bin  $i$  in  $V$ , the calculated cross sections were parametrized according to  $[d\sigma(\alpha_s(M_Z))/dV]_i = C_{1,i} \cdot \alpha_s(M_Z) + C_{2,i} \cdot \alpha_s^2(M_Z)$ . The best combined fit ( $\chi^2 = 2.1$  for 4 data points) was achieved for  $Q^2 > 500 \text{ GeV}^2$  resulting in  $\alpha_s(M_Z) = 0.1212 \pm 0.0017(\text{stat}) +0.0034/ -0.0045$  of the data.

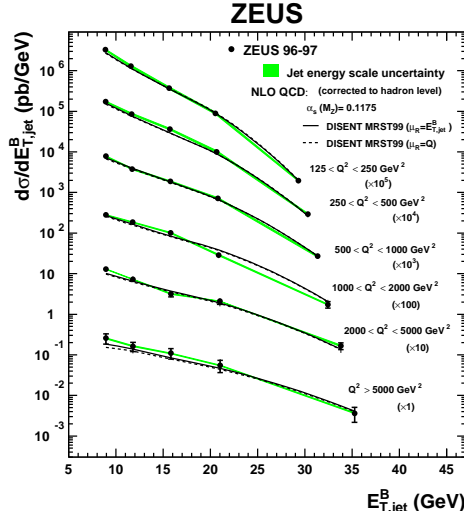


Figure 4: Inclusive jet cross section in DIS as fct. of the transverse jet energy in the Breit system  $E_{TjB}$ .

The energy scale dependence of  $\alpha_s$  has been investigated using the same procedure but parametrizing the measured cross section in terms of  $\alpha_s(\langle E_{T,jB}^B \rangle)$ , where  $\langle E_{T,jB}^B \rangle$  is the mean value of  $E_{T,jB}^B$  in each bin;  $\mu_R = E_{T,jB}^B$  was chosen here since it provides the better description of these data. Good agreement with the predicted running of  $\alpha_s$  is found over a large range of  $E_{T,jB}^B$ .

These data have also been used to study the azimuthal distribution of jets in the Breit frame [3]. At LO, the dependence of the cross section on the angle  $\phi_j^B$  between the lepton scattering plane and jets produced with high  $E_T$  takes the form

$$\frac{d\sigma}{d\phi_j^B} = A + B \cos \phi_j^B + C \cos 2\phi_j^B \quad (3)$$

where the coefficients  $A, B, C$  result from the convolution of the matrix elements for the partonic processes with the PDFs of the proton. The  $\cos \phi$ -term arises from the interference between the transverse and longitudinal components of the exchanged photon (for  $Q^2 \ll M_Z^2$ ) whereas the  $\cos 2\phi$ -term results from the interference of the  $+1/-1$ -helicity amplitudes of its transversely polarized part; nonperturbative contributions arising from intrinsic transverse momenta of the partons have

shown to be small and are negligible at high  $E_T$ . The measured normalized azimuthal distribution shown in fig. 5 is well reproduced by NLO calculations with either  $\mu_R = E_T$  or  $Q$ .

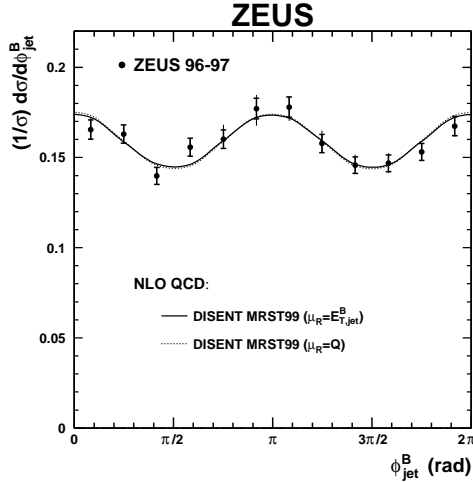


Figure 5: Normalized differential cross section for inclusive jet production in DIS with  $E_{TB_j} > 8$  GeV and  $-2 < \eta_{B_j} < 1.8$ ; inner errors for statistical, outer errors for combined statistical and systematic errors.

H1 has extended the inclusive jet measurements to low  $Q^2$  values of  $5 \text{ GeV}^2 < Q^2 < 100 \text{ GeV}^2$  for  $0.2 < y < 0.6$ ,  $E_T > 5$  GeV and  $-1 < \eta_{\text{lab}} < 2.8$  [4]. The differential cross section as a function of  $E_T$  is shown in fig. 6 for three bins of  $\eta$ . The good agreement with NLO QCD predictions (for  $\mu_R = E_T$ ) found for the backward and central region is getting worse in the forward region i.e. of  $\eta > 1.5$ , and for  $E_T < 20$  GeV, where NLO corrections and uncertainties are becoming larger. For most of the data the theoretical uncertainties (given by the renormalization scale uncertainty) are larger than the experimental errors. Investigating the  $Q^2$  dependence of this discrepancy, it was found to originate from the  $Q^2 < 20 \text{ GeV}^2$  region, indicating that NLO QCD works reasonably well even in the forward region  $\eta_{\text{lab}} > 1.5$  as long as both  $E_T$  and  $Q^2$  are not too small.

In the forward direction, jet production is expected to be sensitive to the dynamics of the parton cascade at small  $x$ . As suggested by Mueller-Navelet, the contribution of DGLAP evolution to DIS should be suppressed by demanding of the forward jet  $E_T^2 \approx Q^2$  while that of BFKL evolution should be enhanced by keeping  $x_j$  as large as feasible and  $x/x_j$  small.

H1 has taken data on inclusive jet production in the forward direction [5] i.e.  $7^\circ < \Theta_{j\text{lab}} < 20^\circ$  with  $0.5 < Q^2/E_T^2 < 2$  and  $x_j > 0.035$  ( $E_T > 3.5$  GeV). The measurement and jet search with the ILICA is

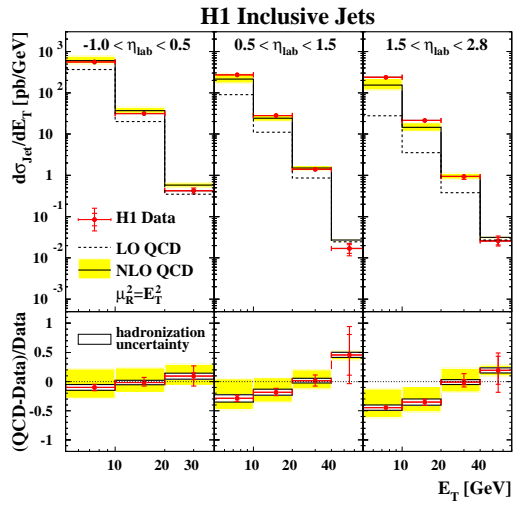


Figure 6: Inclusive jet cross section  $d\sigma/dE_T$  in DIS integrated over  $5 \text{ GeV}^2 < Q^2 < 100 \text{ GeV}^2$  and  $0.2 < \eta_{\text{lab}} < 0.6$  as function of the transverse jet energy  $E_T$  in the Breit system for different ranges of  $\eta_{\text{lab}}$ : forward (proton direction):  $1.5 < \eta < 2.8$ ; central:  $0.5 < \eta < 1.5$ ; backward:  $-1.0 < \eta < 0.5$ . NLO QCD model: DISSENT with CTEQ5M (solid line) and no hadronization corrections; hatched band: change of the renormalization scale by  $1/2$  and  $2$ .

performed in the lab frame with cuts  $5 < Q^2 < 75 \text{ GeV}^2$  and  $0.1 < y < 0.7$ . The data (fig. 7) are compared with four different Monte Carlos. The differential cross sections in  $x$  and  $x_j$  are up to a factor of two larger than the DGLAP prediction for direct photons only (RG (DIR)), but they are reasonably well described if a resolved photon is included. The description provided by the CDM model is also good while CCFM predicts too large cross sections.

In forward  $\pi^0$  production, the parton is tagged by a single energetic fragmentation product. While smaller forward angles than in jet production can be reached, the cross sections are lower and the hadronization uncertainties higher.

Inclusive  $\pi^0$ -production in DIS has been measured by H1 [6], with the following cuts:  $0.1 < y < 0.6$ ,  $4.10^{-5} < x < 6.10^{-3}$ ,  $2 \text{ GeV}^2 < Q^2 < 70 \text{ GeV}^2$  and  $\pi^0$  cms-momenta  $> 2.5$  GeV, polar angles of  $5^\circ < \Theta_\pi < 25^\circ$  (corresponding to the central region in the hadronic cms) and  $x_\pi > 0.01$ ; no explicit cut on  $p_{T\pi^0}^2/Q^2$  was applied. In fig. 8, the differential cross section is compared with QCD-based models. The DGLAP prediction with direct photon interaction only is too low, but the inclusion of resolved photon interaction - albeit with a choice of the renormalization and factorization scale different ( $Q^2 + 4p_T^2$ ) than in forward jet production - yields a good description. BFKL based calculation also describes the data reasonably well, while CCFM evolution fails at small  $x$ .

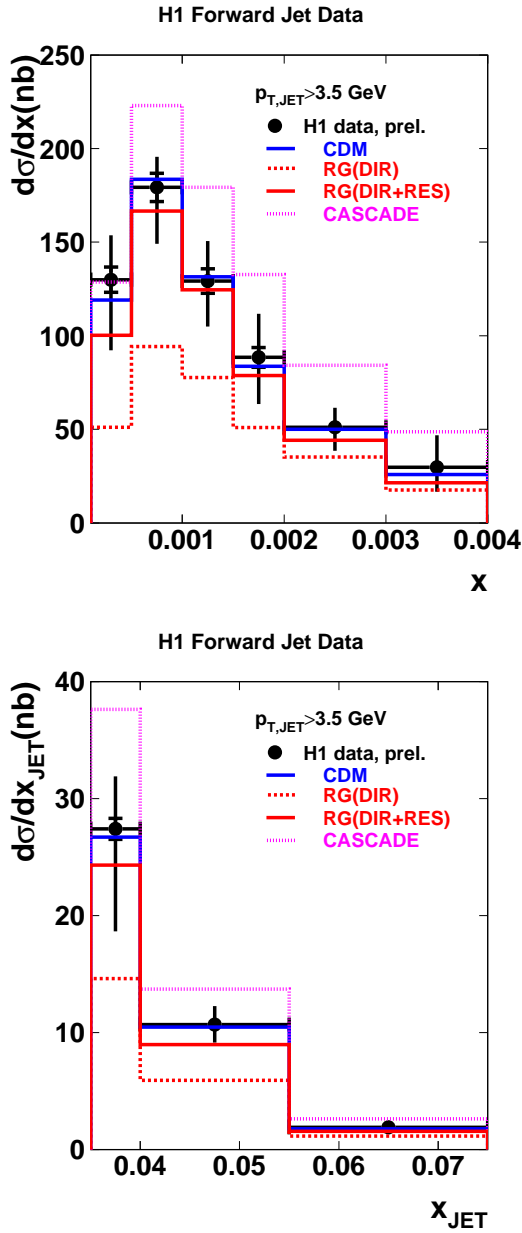


Figure 7: Inclusive forward jet cross sections in DIS for  $p_{tj} > 3.5$  GeV;  $7^\circ < \Theta_j < 20^\circ$ ;  $x_j > 0.035$  at the hadron level. Models: CDM (Color-Dipole-Model: DJANGO + ARIADNE), RG (RAPGAP: DIRECT and DIRECT + RESOLVED), CASCADE (CCFM). Data are preliminary.

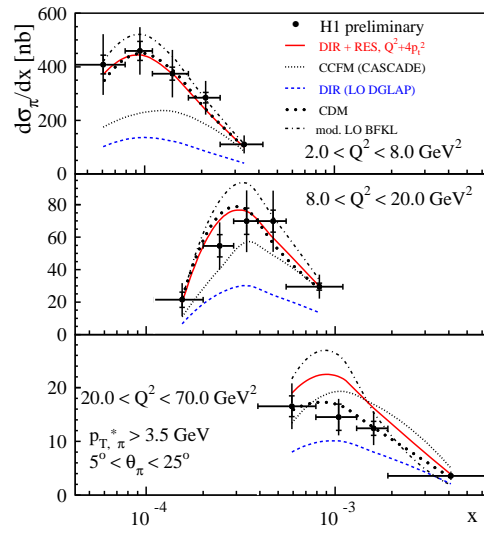


Figure 8: Inclusive forward  $\pi^0$  cross section in DIS for transverse momenta in the  $\gamma$ -proton cms  $p_{T\pi^0}^* > 3.5$  GeV and  $5^\circ < \Theta_{\pi^0} < 25^\circ$  for different ranges of  $Q^2$ . Models: DIR (RAPGAP for DIRECT proc.), DIR + RES (RAPGAP for DIRECT + RESOLVED proc.), CCFM (CASCADE), CDM (Color-Dipole-Model: ARIADNE), mod. LO BFKL (modified LO BFKL evolution).

In a recent measurement by ZEUS [7] of inclusive jet production in DIS for  $Q^2 > 25$  GeV<sup>2</sup>,  $y > 0.4$  and with  $E_{Tj} > 6$  GeV,  $-1 < \eta_j < 3$ , deviations of the data from NLO QCD predictions calculated in the lab frame to  $O(\alpha_s^1)$  were found to increase towards the forward direction (fig. 9, upper part) and small  $E_{Tj}$ ,  $Q^2$  and  $x$ . In a further analysis of these data, the Mueller-Navelet suggestion was applied by combining the detection of a hard forward jet ( $E_{Tj} > 6$  GeV,  $0 < \eta_j < 3$ ) with requiring the hadronic angle  $\gamma_{\text{hadr}}$ , corresponding to the direction of the scattered quark in the QPM, to be reconstructed in the backward direction of the detector ( $\cos \gamma_{\text{hadr}} < 0$ ) and thus suppressing QPM contributions to the forward jets. Comparing the cross sections for such defined jet configurations ("dijet phase space") with NLO QCD predictions calculated to  $O(\alpha_s^2)$ , better agreement (fig. 9, lower part) is found in the forward direction at the expense of a considerably larger uncertainty in the renormalization scale which swamps a possible BFKL signal in this part of the phase space.

## 2.2 Dijets

The LO QCD processes which contribute to dijet production in DIS are QCD Compton scattering (QCDC) and boson-gluon-fusion (BGF). In the high  $Q^2$  region, where the QCDC process is dominant and the PDFs are well constrained by fits to inclusive DIS data, dijet measurements with  $\alpha_s$  as

input enable tests of pQCD; at low  $Q^2$ , where BGF dominates, the comparison of measured dijet cross sections with QCD predictions for different PDFs has been used to investigate the gluon density distribution.

In dijet measurements by H1 [1] and ZEUS [8] asymmetric cuts in  $E_T$  have been applied to the two jets highest  $E_T$  in the Breit system in order to avoid regions of the dijet phase space which are sensitive to soft gluon radiation. The data (fig. 10) are compared with DISSENT NLO calculations, which have been checked with MEPJET. For  $O(10) \text{ GeV}^2 < Q^2 < O(10.000) \text{ GeV}^2$  and  $E_{TB} > 5 \text{ GeV}$ , i.e. where NLO and hadronization corrections are small, the studied jet observables are reproduced within about 10%; for  $Q^2 < 10 \text{ GeV}^2$ , however, where NLO corrections are becoming large, significant disagreement is observed. (For new data on multijet production by ZEUS see Chap. 2.3.)

From the dijet fraction  $R_{2+1}(Q^2)$  measured by ZEUS,  $\alpha_s$  was determined using the same method as applied to inclusive jets (Chap. 2.1) with the result  $\alpha_s(M_Z) = 0.1166 \pm 0.0019(\text{stat}) + 0.0024/0.0033(\text{exp}) + 0.0057/-0.0044(\text{theor})$ . Also the dependence of  $\alpha_s$  on the scale  $Q$  is in good agreement with expectations.

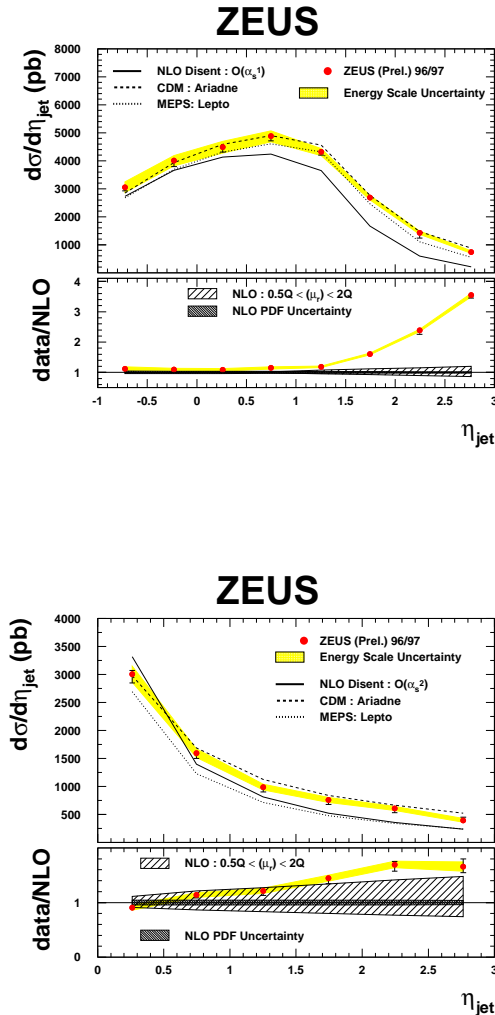


Figure 9: Upper figure: Inclusive jet cross sections in DIS for  $Q^2 > 25 \text{ GeV}^2$ ,  $y > 0.04$ ,  $E_{Tj} > 6 \text{ GeV}$  and  $-1 < \eta_j < 3$  in comparison to  $O(\alpha_s^1)$ -NLO QCD calculations in the lab frame ("inclusive phase space", see text). Lower figure: Jet cross sections for the same kinematical conditions but constraining the jet topology to  $\eta_j > 0$  and  $\cos \gamma_{hadr} < 0$  in comparison with  $O(\alpha_s^2)$ -NLO QCD calculations in the lab frame ("dijet phase space").

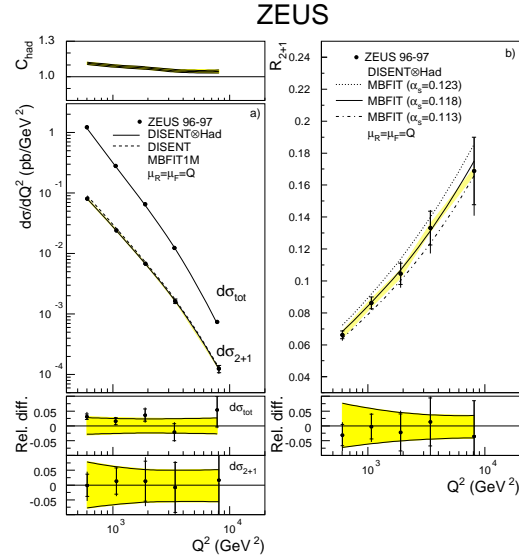


Figure 10: (left) Inclusive jet ( $\sigma_{tot}$ ) and dijet ( $\sigma_{2+1}$ ) cross sections in DIS, hadroniz. corr.  $C$  refers to dijets; (right): dijet fraction  $R_{2+1}$ , shaded band gives uncertainty of abs. energy scale of jets.

Recently, low  $x$  dijet production has been studied in more detail by H1 [9] in the kinematic region  $5 \text{ GeV}^2 < Q^2 < 100 \text{ GeV}^2$ ,  $10^{-4} < x < 10^{-2}$  and  $0.1 < y < 0.7$ . For jets reconstructed in the hadronic cms with cuts of  $E_{T1} > 7 \text{ GeV}$ ,  $E_{T2} > 5 \text{ GeV}$  within  $-1 < \eta < 2.5$ , the triple differential dijet cross sections in  $(x, Q^2, E_{Tmax})$  (fig. 11) and

( $x, Q^2, \Delta\eta$ ) do not show significant deviations from NLO calculations with  $\mu_R = (E_{T1} + E_{T2})/2$ ,  $\mu_F = \sqrt{\langle E_T^2 \rangle} = \sqrt{70 \text{ GeV}^2}$ , in contrast to the ratio of the number of dijet events with azimuthal angle separation of less than  $120^\circ$  to all dijet events (fig. 12). Better agreement for part of the phase space can be achieved by combining LO ME with direct photon processes and  $k_T$  ordered parton emission.

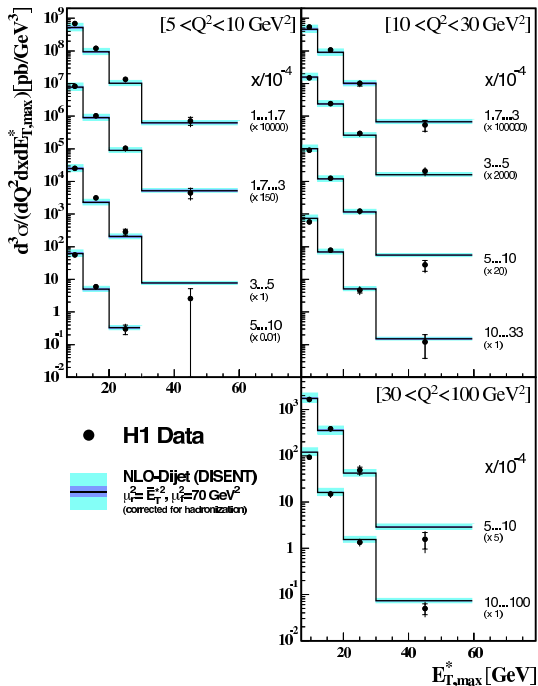


Figure 11: Inclusive dijet cross section in DIS for  $10^{-4} < x < 10^{-2}$  as a function of the maximum transverse jet energy  $E_{T,\text{max}}^*$  in the hadronic cms compared to NLO QCD predictions (for CTEQ5M) corrected for hadronization. Outer light error band includes hadronization (dark band) and renorm. scale uncertainties.

## 2.3 Trijets

While the cross sections for inclusive jet and dijet production in LO pQCD depend on  $O(\alpha_s)$  only, the trijet cross section already in LO is sensitive to  $O(\alpha_s^2)$ .

Trijet production in DIS has been measured by H1 [10] for  $5 \text{ GeV}^2 < Q^2 < 5000 \text{ GeV}^2$ , selecting jets with  $E_T > 5 \text{ GeV}$  in the Breit frame. The measured cross sections (fig. 13) were compared with LO and NLO calculations using NLOJET with  $\mu_R$  and  $\mu_F$  set to the average transverse energy  $\overline{E_T}$  of the 3 jets in the Breit frame; for the proton PDFs CTEQ5M1 was taken with  $\alpha_s(M_Z) = 0.118$ . The inclusive trijet cross sections for invariant masses  $> 25 \text{ GeV}$  as well as the trijet/dijet ratio, in which many theoretical and experimental uncertainties cancel out, agree well with the NLO predictions in spite of the large NLO corrections. Also the angu-

lar distribution of trijets agrees well with the pQCD expectation.

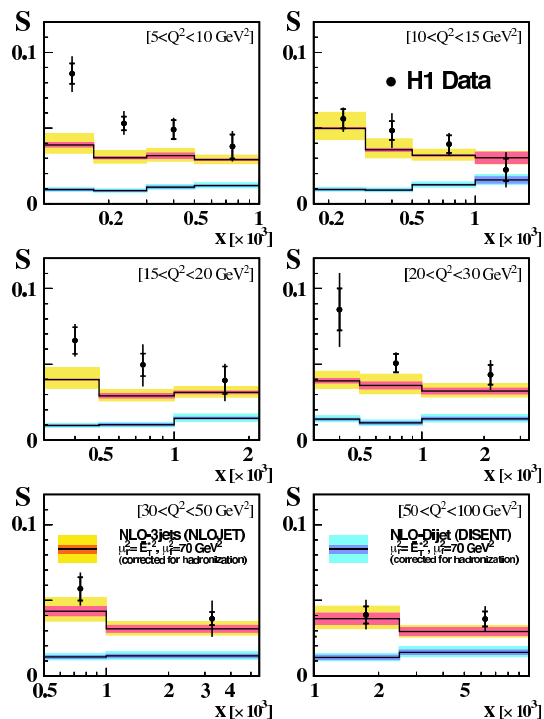


Figure 12: Ratio  $S$  of number of dijet events with small azimuthal jet separation ( $\phi < 2\pi/3$ ) to the total number of inclusive dijet events as a function of (Bjorken) $x$  compared to NLO QCD predictions and with error bands as in fig. 12.

Recent studies of dijet and trijet production by ZEUS [11] for  $10 \text{ GeV}^2 < Q^2 < 5000 \text{ GeV}^2$  in the kinematic range  $0.04 < y < 0.6$ ,  $\cos \gamma_{\text{hadr}} < 0.7$ , with cuts in the jet phase space of  $-1 < \eta_{\text{lab}} < 2.5$ ,  $E_{TB} > 5 \text{ GeV}$  for invariant masses of  $M_{2j,3j} > 25 \text{ GeV}$  are shown in figs. 14 and 15. Good agreement is found with the pQCD predictions after correcting for hadronization, i.e. to  $O(\alpha_s^3)$ .

## 2.4 Subjet multiplicities

Reapplication of the jet algorithm with smaller resolution scale  $y_{\text{cut}}$  to identified jets allows the resolution of clusters within the jets which are called subjets. The development of the subjet multiplicity with  $y_{\text{cut}}$  can be calculated in pQCD for high  $E_{Tj}$  and not too low  $y_{\text{cut}}$  values, i.e. where fragmentation effects are estimated to be small in NLO. Since the subjet multiplicity is mainly determined by QCD radiation in the final state, it only weakly depends on the PDFs of the proton.

The mean subjet multiplicity has been measured by ZEUS [12] in NC DIS processes with  $Q^2 > 125 \text{ GeV}^2$  for  $E_T > 15 \text{ GeV}$  and  $-1 < \eta_j < 2$ . The ILICA was applied to jets in the lab frame, where calculations of up to  $O(\alpha_s^2)$  can be performed. The mean subjet multiplicity  $\langle n_{\text{sbj}} \rangle$  was determined

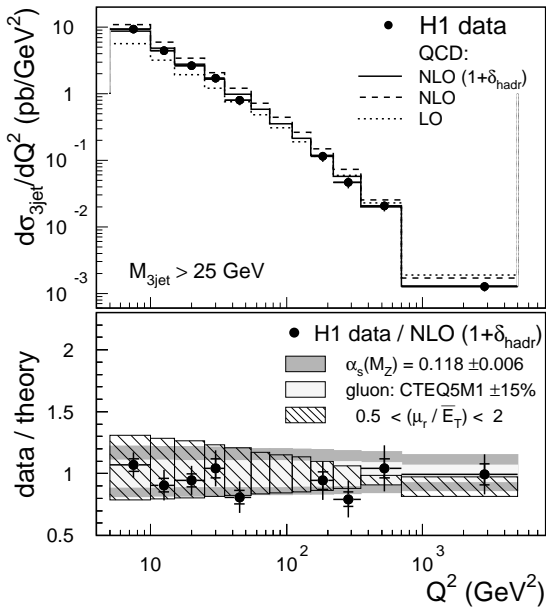


Figure 13: Inclusive trijet production in DIS for  $5 \text{ GeV}^2 < Q^2 < 5000 \text{ GeV}^2$ ;  $-1 < \eta_{\text{lab}} < 2.5$ ;  $M_{3j} > 24 \text{ GeV}$ . QCD: NLOJET.

for  $5 \cdot 10^{-4} < y_{\text{cut}} < 0.1$ . The data are in good agreement with NLO calculations with  $\mu_R = \mu_F = Q$  using the CTEQ4M PDFs. (fig. 16).

Using the method described earlier (see Chap. 2.1),  $\alpha_s$  was determined from these data for  $25 \text{ GeV} < E_T < 71 \text{ GeV}$  and  $y_{\text{cut}} = 10^{-2}$  yielding  $\alpha_s(M_Z) = 0.1187 \pm 0.0017(\text{stat}) + 0.0024 / - 0.0009(\text{syst}) + 0.0093 / - 0.0076(\text{theor})$ . While the experimental uncertainty is comparable to that resulting from jet measurements, the theoretical uncertainty is larger and dominated by NNLO terms.

### 3 Jets in high energy photo-production

In LO QCD direct as well as resolved processes (c.f. Chap. 1) have to be considered in the calculation of the jet cross section. If  $x_\gamma$  is the fractional momentum of parton  $a$  of the photon and  $x_p$  the same of parton  $b$  of the proton, the jet cross section is obtained from the convolution of the photon PDF  $f_{\gamma b}(x_\gamma, \mu^2)$  and the proton PDF  $f_{pa}(x_p, \mu^2)$  with the hard partonic cross section  $d\sigma_{a,b}(x_\gamma, x_p, \alpha_s, \mu^2)$

$$\sigma_j = \sum_{a,b} \int \int dx_\gamma dx_p f_{pa}(x_p, \mu^2) f_{\gamma b}(x_\gamma, \mu^2) \cdot d\sigma_{a,b}(x_p, x_\gamma, \alpha_s, \mu^2) \cdot (1 + \delta_{\text{hadr}}) \quad (4)$$

summed over all partons  $a, b$  from the photon and proton. For direct photon interactions  $f_\gamma$  is a  $\delta$ -function at  $x_\gamma = 1$ . Since the transverse energy  $E_T$

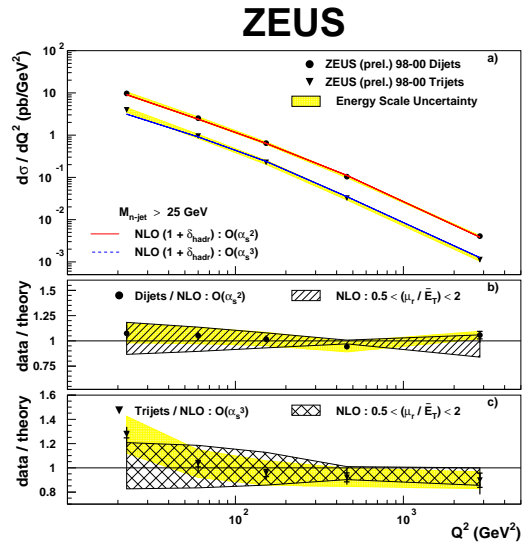


Figure 14: Inclusive dijet and trijet cross section in DIS. The light shaded band indicates the calorimeter energy scale uncertainty, the hatched band the renormalization scale uncertainty.

of the jet or jet system is the only scale parameter available in the photoproduction of jets from light quarks,  $\mu_R$  and  $\mu_F$  are set to  $\mu_R = \mu_F = \mu = E_T$ . In resolved processes photon fragments may interact with proton remnants causing a background of multiparton interactions ("underlying events"), which has to be corrected for; it remains below 10% for  $E_T > 20 \text{ GeV}$ .

At HERA, the proton PDFs are, with the current statistics, predominantly probed in the range  $0.05 < x_p < 0.5$ , where they are well constrained by measurements of  $F_2^p$ . For the photon PDFs the probed range is  $0.1 < x_\gamma < 1$  in which quarks are well constrained for  $x_\gamma < 0.5$  by measurements of  $F_2^\gamma$  at LEP, while the gluon is only poorly constrained. Since jet production at HERA is sensitive to the gluon component in the photon at LO, it should allow to extend the study of the photon structure to higher scales.

In single jet production, in comparison to dijet production, an increased kinematic range is accessible, higher statistical accuracy can be achieved and infrared dangerous regions of phase space are not existent; on the other hand single jet photoproduction is less sensitive to details of the hard scattering process.

#### 3.1 Inclusive jets

H1 [13] and ZEUS [14] have performed similar measurements and analyses of inclusive jet cross sections for photons of  $Q^2 < 1 \text{ GeV}^2$  within  $-1 < \eta_j < 2.5$ . The H1 data for  $E_T > 21 \text{ GeV}$  cover a range of the hadronic cms-energy  $W_{\gamma p}$  of  $95 \text{ GeV} < W_{\gamma p} <$

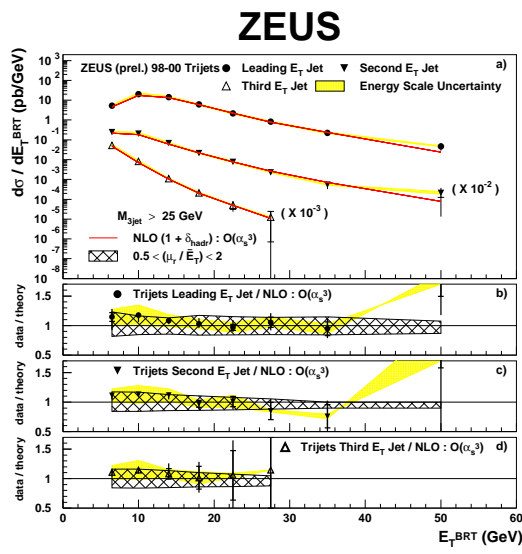


Figure 15: Inclusive trijet cross section in DIS; error bands as in fig. 14.

285 GeV. The measurements were extended down to  $E_T > 5$  GeV with a dedicated trigger for photons of  $Q^2 < 0.01$  GeV<sup>2</sup> in the restricted kinematic range of  $164 \text{ GeV} < W_{\gamma p} < 242$  GeV. The ZEUS data were taken for  $142 \text{ GeV} < W_{\gamma p} < 293$  GeV for  $E_T > 17$  GeV (see fig. 17). H1 compares the data with the NLO QCD calculations of Frixione and Ridolfi, using CTEQ5M1 for the proton PDFs and GRV for the photon PDFs and setting  $\mu_R = \mu_F$  to the average transverse energy of the two outgoing partons; ZEUS compares with Klasen, Kleinwort, Kramer, using MRST99 for the proton and GRV for the photon with  $\mu_R = \mu_F = E_{Tj}$ . In both analyses good agreement with NLO QCD over six orders of magnitude of the cross section is found; the H1 data for  $Q^2 < 0.01$  GeV and  $5 \text{ GeV} < E_T < 12$  GeV may indicate a cross section rising above prediction with increasing  $\eta$ .

From the ZEUS data,  $\alpha_s(M_Z)$  was determined (see Chap. 2.1) by calculating in NLO QCD for each  $E_T$ -bin  $i$  the cross section  $(d\sigma/dE_T)_i$  using the three sets of MRST99 with their corresponding  $\alpha_s(M_Z)$ -values. By combining the  $\alpha_s$  values for the different  $E_T$  bins a value of  $\alpha_s = 0.1224 \pm 0.0002(\text{stat}) + 0.0022/ - 0.0019(\text{exp}) + 0.0054/ - 0.0019(\text{theor})$  was obtained. The major error sources are the jet energy scale ( $\pm 1.5\%$  in  $\alpha_s(M_Z)$ ) and the renormalization scale ( $+4.2/ - 3.3\%$  in  $\alpha_s(M_Z)$ ); the uncertainties from the PDFs and hadronization are estimated to be less than 1%.

Similarly, the dependence of  $\alpha_s$  on the energy scale was investigated by determining  $\alpha_s$  from  $d\sigma/dE_T$  at different  $E_T$  values. The resulting  $\alpha_s(E_T)$  values agree well with the predicted running of  $\alpha_s$ .

Using the above data, ZEUS has measured the

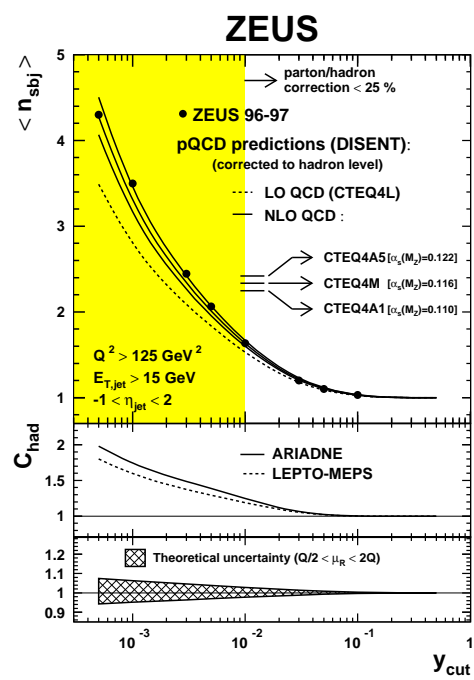


Figure 16: Mean subjet multiplicity as a function of  $y_{\text{cut}}$  in inclusive jet production in DIS for  $E_{Tj} > 15$  GeV,  $Q^2 > 125$  GeV<sup>2</sup> and  $-1 < \eta_j < 2$ .

dependence of the scaled invariant jet cross sections  $E_{Tj}^4 E_j d^3\sigma/dp_{xj} dp_{yj} dp_{zj}$  on the dimensionless variable  $x_T = 2E_{Tj}/W_{\gamma p}$ . The cross section measured at  $\langle W_{\gamma p} \rangle$  of 180 and 255 GeV and averaged over  $-2 < \eta_j^{\gamma p} < 0$ , agrees well with NLO QCD. In the quark parton model, the scaled cross section should be independent of  $W_{\gamma p}$ , whereas from QCD one expects a violation of scaling due to the evolution of the structure functions and the running of  $\alpha_s$ . As shown in fig. 18, the ratio of the scaled cross section at the two different energies  $W_{\gamma p}$  violates scaling as predicted by NLO QCD.

### 3.2 Inclusive dijets

Dijet production has been measured by ZEUS [15] and H1 [16] under similar kinematical conditions as in single jet production. In both experiments the jets were reconstructed with the ILICA, requiring asymmetric cuts on  $E_T$  in the lab frame. Both experiments cover a range of  $-1 < \eta_{j1,2} < 2.5$  and  $0.1 < y < 0.9$ . The quantity  $x_\gamma^{\text{obs}}$  is introduced

$$x_\gamma^{\text{obs}} = (E_{Tj1}e^{-\eta_1} + E_{Tj2}e^{-\eta_2})/2yE_e \quad (5)$$

where  $y = W^2/s$ , which in LO corresponds to the fraction of the photon momentum that contributes to the production of the two highest- $E_T$  jets; cuts on  $x_\gamma^{\text{obs}}$  allow the data sample to be enriched with direct processes (high  $x_\gamma^{\text{obs}}$ ) or resolved processes (low  $x_\gamma^{\text{obs}}$ ). The measurements are compared to

NLO QCD calculations with  $\mu_R = \mu_F$  equal set to the average  $E_T$  of the two outgoing partons. The PDF-parametrizations used are GRV-HO and AFG-HO for the photon and CTEQ5M1 for the proton;  $\alpha_s(M_Z)$  is set to 0.118.

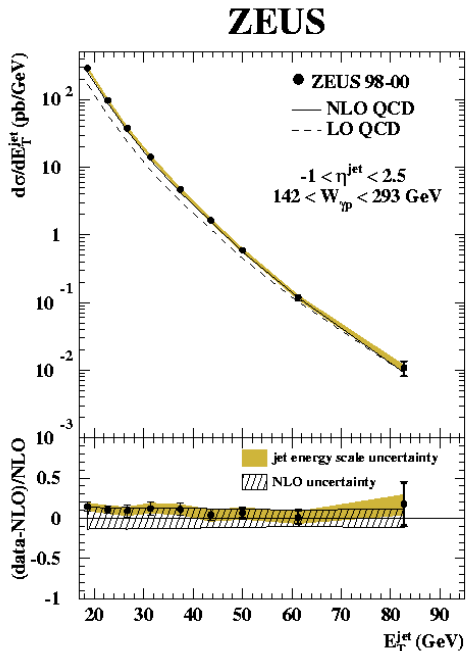


Figure 17: Inclusive jet production in photoproduction ( $Q^2 < 1 \text{ GeV}^2$ ) integrated over  $-1 < \eta_j < 2.5$ . LO and NLO: Klasen, Kleinwort, Kramer with  $\mu_R = \mu_F = E_T$ , proton-PDFs: MRST99, photon-PDFs: GRV.

The measured angular distributions (fig. 19) confirm the steeper rise expected for resolved photon processes ( $x_\gamma^{obs} < 0.75$ ) in comparison to direct photon processes ( $x_\gamma^{obs} > 0.75$ ), indicating that the dynamics of the hard scattering process is reasonably well described. For the H1 data, the cross section as a function of  $x_\gamma$  (here identical to  $x_\gamma^{obs}$ ), shown in fig. 20 for two regions of  $E_{T,max}$ , which represent two different factorization scales for the PDFs of the proton and photon, agrees with NLO predictions and varies only slightly with the different parametrizations of the photon PDFs while ZEUS observes differences; it has to be noted, however, that the different  $E_T$ -cuts have been used (H1:  $E_{T1} > 25 \text{ GeV}$ ,  $E_{T2} > 15 \text{ GeV}$ ; ZEUS:  $E_{T1} > 14 \text{ GeV}$ ,  $E_{T2} > 11 \text{ GeV}$ ).

## 4 Summary of results on $\alpha_s$

The results obtained from the recent measurements of jet and subjet cross sections in DIS and photoproduction on  $\alpha_s(M_Z)$  as well as on the scaling behaviour of  $\alpha_s$  have achieved an accuracy compatible with results from other colliders. They are also

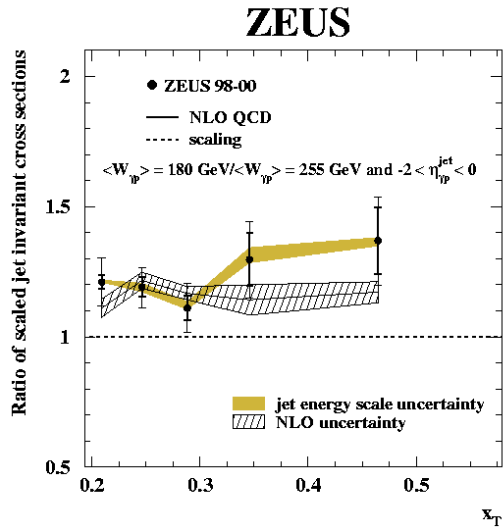


Figure 18: Scaling violation in photoproduction ( $Q^2 < 1 \text{ GeV}^2$ ): Ratio of measured scaled invariant jet cross sections (see text) for the two  $\langle W_{\gamma p} \rangle$  shown and averaged over  $-2 < \eta_j^p < 0$ . NLO QCD as in fig. 17.

in good agreement with the world average (figs. 21 and 22).

## 5 Summary

For large scales,  $Q^2$  and/or jet- $E_T$ , the recent results from H1 and ZEUS on jet production in deep inelastic scattering and photoproduction are in good agreement with NLO QCD. In general, the hadronization corrections applied to the NLO results are small and improve the description of the data only slightly. For decreasing scales and in specific areas of phase space the corrections become large and are important in improving the description of the data.

In these studies, the longitudinally invariant  $k_T$  cluster algorithm in its inclusive mode has proved reliable and, therefore, become the preferred method of jet identification in this field. The good agreement of  $\alpha_s$  determinations performed with jet (and subjet) production at high  $Q^2$  and  $E_T$  with the world average supports this conclusion.

The situation is worse in the small  $x$  / forward region. For  $x < 10^{-4}$  and small  $Q^2$  a breakdown of DGLAP is to be expected and indeed increasing discrepancies with DGLAP based predictions are observed even in NLO. In some cases in spite of small experimental errors the sizable theoretical uncertainties, however, do not yet allow safe conclusions on a more satisfactory and comprehensive description of the data by modified pQCD models like BFKL or CCFM.

Not only an improvement of experimental statistical and systematic errors, to come from HERA

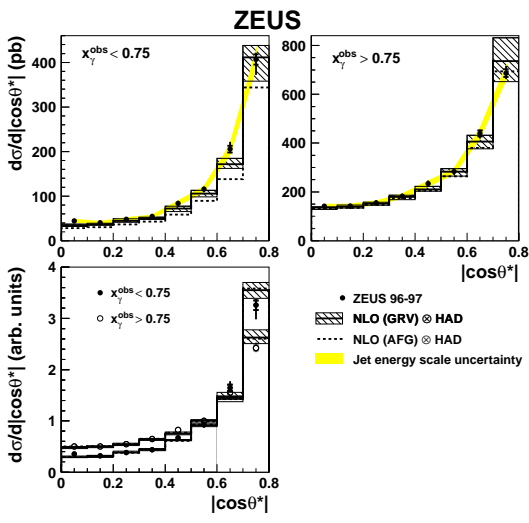


Figure 19: Inclusive dijet production in photoproduction ( $Q^2 < 1 \text{ GeV}^2$ ) as a function of the dijet angle  $\Theta^*$  in the parton-parton-cms for different cuts on the fractional momentum  $x_\gamma^{\text{obs}}$  of the photon participating in the production of the two jets with the highest transverse energy. Cuts:  $E_{Tj1,2} > 14, 11 \text{ GeV}$ ;  $-1 < \eta_j < 2.4$ ;  $134 < W_{\gamma p} < 277 \text{ GeV}$ . NLO: Frixi-one, Ridolfi with CTEQ5M for proton-PDFs and GRV resp. AFG for photon-PDFs.

II, but also more accurate model calculations are needed to get closer to a satisfactory understanding of the interplay of soft and hard QCD processes in DIS and photoproduction.

#### Acknowledgement:

My thanks are due to P.N. Bogolyubov and L. Jenkovsky for the invitation to an interesting and enjoyable conference. I am indebted to G. Grindhammer for valuable discussions and to him as well as to T. Greenshaw for a critical reading of the paper. I also thank Kristiane Preuss and Marlene Schaber for their technical help with the paper.

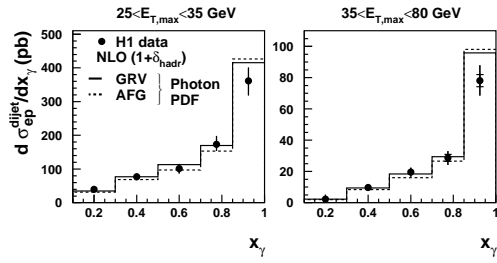


Figure 20: Inclusive dijet production in photoproduction ( $Q^2 < 1 \text{ GeV}^2$ ) as function of the fractional momentum  $x_\gamma$  of the photon participating in the production of the two jets with highest transverse energy  $E_T$  (identical to  $x_\gamma^{\text{obs}}$  in fig. 20). Cuts:  $E_{Tj1,2} > 25, 15 \text{ GeV}$ ;  $-0.5 < \eta_j < 2.5$ ;  $95 < W_{\gamma p} < 285 \text{ GeV}$ . QCD, PDFs as in fig. 19.

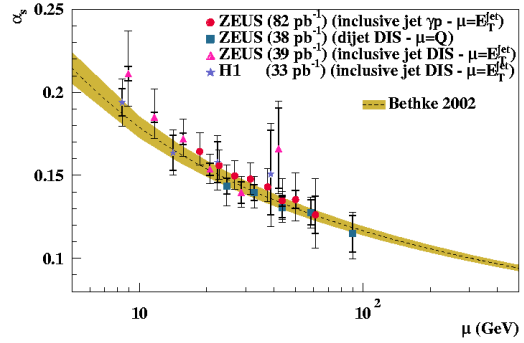


Figure 21: Scale dependence of  $\alpha_s$  from recent HERA experiments.

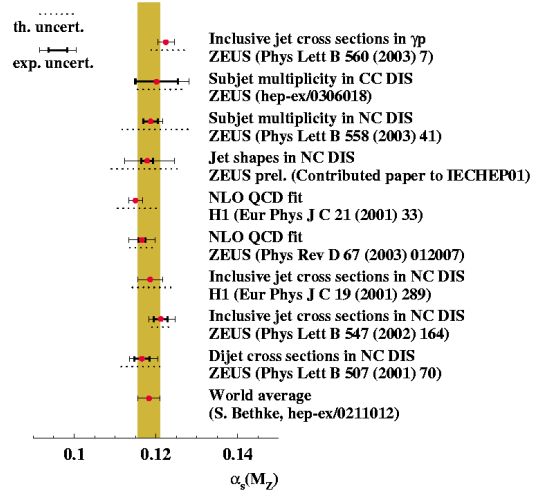


Figure 22: Determination of  $\alpha_s(M_Z)$  and its scale dependence in recent HERA experiments.

## References

- [1] Adloff, C. et al.: *Europ. Phys. J.* **C19** (2001), 289. DESY 00-145; hep-ex/0010054.
- [2] Chekanov, S. et al.: *Physics Letters* **B547** (2002) 164. DESY 02-112; hep-ex/0208037.
- [3] Chekanov, S. et al.: *Physics Letters* **B551** (2003) 226. DESY 02-171; hep-ex/0210064.
- [4] Adloff, C. et al.: *Physics Letters* **B542** (2002) 193. DESY 02-079; hep-ex/0206029.
- [5] Jung, J.: H1 Collaboration, ICHEP 02, Amsterdam (2002).
- [6] Goerlich, L.: H1 Collaboration, DIS 2003, St. Petersburg (2003).
- [7] Lammers, S.: ZEUS Collaboration, DIS 2003, St. Petersburg (2003).
- [8] Breitweg, J. et al.: *Physics Letters* **B507** (2001) 70. DESY 01-018; hep-ex/0102042.  
Chekanov, S. et al.: *Europ. Phys. J.* **C23** (2002) 13. DESY 01-127; hep-ex/0109029.
- [9] Poeschl, R.: H1 Collaboration, DIS 2003, St. Petersburg (2003).
- [10] Adloff, C. et al.: *Physics Letters* **B515** (2001) 17. DESY 01-073; hep-ex/0106078.
- [11] Krumnack, N.: ZEUS Collaboration, DIS 2003, St. Petersburg (2003).
- [12] Chekanov, S. et al.: *Physics Letters* **B558** (2003) 41. DESY 02-217; hep-ex/0212030.
- [13] Adloff, C. et al.: submitted to *Europ. Phys. J.* **C**. DESY 02-225; hep-ex/0302034.
- [14] Chekanov, S. et al.: *Physics Letters* **B560** (2003) 7. DESY 02-228; hep-ex/0212064.
- [15] Chekanov, S. et al.: *Europ. Phys. J.* **C23** (2002) 61. DESY 01-220; hep-ex/0112029.
- [16] Adloff, C. et al.: *Europ. Phys. J.* **C25** (2002), 13. DESY 01-225; hep-ex/0201006.